International Journal of Concrete Structures and Materials
Vol.18, No.3E, pp.191~198, December 2006

Fracture Characteristics of Concrete at Early Ages

Yun Lee[1] and Jin-Keun Kim[2]

(Originally published in Korean version of ***Journal of KCI***, Vol.14, No.1, January 2002)

Abstract: The objective of this study is to examine fracture characteristics of concrete at early ages, i.g. critical stress intensity factor, critical crack-tip opening displacement, fracture energy, and bilinear softening curve based on the concepts of effective-elastic crack model and cohesive crack model. A wedge splitting test for Mode I was performed on cubic wedge specimens with a notch at the edge. By experimenting with various strengths and ages, load-crack mouth opening curves were obtained, and the results were analyzed by linear elastic fracture mechanics and FEM (finite element method). The results from the test and analysis showed that critical stress intensity factor and facture energy increased while critical crack-tip opening displacement decreased with concrete aging from 1 day to 28 days. Four parameters of bilinear softening curve from 1 day to 28 days were obtained from a numerical analysis. The obtained fracture parameters and bilinear softening curves at early ages from this study are to be used as a fracture criterion and an input data for the finite element analysis of concrete at early ages.

Keywords: critical stress intensity factor, critical crack-tip opening displacement, fracture energy, bilinear softening curve, wedge spitting test, early ages

1. Introduction

The majority of cracks occurring in concrete structures are caused right after the concrete implementation by outside environmental factors such as temperature stress, self-shrinkage, dry shrinkage, etc. These factors are the major reasons for the collapse of the structures at early ages in actual construc-tion sites. Moreover, they can result in not only the cause of cracks in the structures (even before the concrete is completely hardened) but also the deterioration in the overall durability of the structures. Thus, it is necessary to investigate the methods for the control and evaluation of the cracks occurring in the concrete at early ages. This task calls for various experiments on the factors of influence on the crack and a comprehensive analysis of the cracking based on the experimental results. The first step to approach this task could start from the delineation of the fracture characteristics of concrete at early ages. Accordingly, this paper aims to investigate the fracture characteristics of concrete at early ages.

The models to approach the investigation of the concrete fracture can be largely classified into two types.

One is an effective elastic crack model, which applies linear elastic fracture dynamics to brittle materials, and the other is a cohesive crack model, which focuses on the softening of similar brittle materials to trace the progress of fracture. This study aims to delineate those parameters thought as the fracture characteristics of the concrete at early age by investigating critical crack-tip opening displacement ($CTOD_c$) and critical stress intensity factor (K_{Ic}) with effective elastic crack model and fracture energy (G_F)and bilinear softening curve with cohesive crack model.

[1] KCI member, Dept. of Civil Engineering, Korea Advanced Institute of Science and Technology, Daejon 305-701, Korea.
[2] KCI member, Dept. of Civil Engineering, Korea Advanced Institute of Science and Technology, Daejon 305-701, Korea.
E-mail: kimjinkeun@kaist.ac.kr

2. Fracture characteristics of concrete

2.1 Effective elastic crack model

The effective elastic crack model is used to predict the complex fracture behavior of materials with displacement softening property by applying a linear elastic fracture dynamics with an assumption of a fictitious cracked front-end. Generally, the relationship between the actual length of the crack and the effective elastic crack length can be expressed as an effective crack expansion length $\Delta\alpha_e$ as shown in Fig. (1).

$$\Delta a_e = a_e - a_0 \tag{1}$$

where, a_e is the effective elastic crack length, and a_e is the initial length of the crack.

In 1985, Jenq and Shah[1] proposed a two-parameter model, which can theoretically predict the effect of the maximum load on the cracks of random size and shape occurring in test specimens. As seen in Fig. 1, the two-parameter model represents the actual crack caused by the maximum load as a hypothetical and critical effective elastic crack length, a_c, with the assumption that the critical crack-tip opening displacement, $CTOD$, is equal to a certain critical value, $CTOD_c$. In this model, the standard for evaluating the crack progress is represented by two parameters. One is the critical stress intensity factor, K_{Ic}, at the effective crack-tip, and the other is the aforementioned

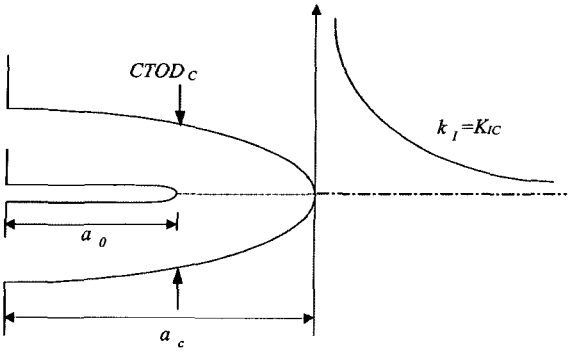

Fig. 1 Effective elastic crack profile and definition of crack-tip opening displacement in 2-parameter model.

$CTOD_c$. Jenq and Shah proposes that the crack will propagate when the stress intensity factor reaches the critical value of K_{Ic} and $CTOD$ reaches the critical value of $CTOD_c$. These two parameters are expressed in Eqs. (2) and (3) below.

$$K_{Ic} = \sigma_c \sqrt{\pi a_c} g_1\left(\frac{a_c}{d}\right) \tag{2}$$

$$CTOD_c = \frac{4\sigma_c a_c}{E} g_2\left(\frac{a_c}{d}\right) g_3\left(\frac{a_c}{d}, \frac{a_0}{a_c}\right) \tag{3}$$

where, σ_c is the critical stress and d is the depth of the test specimen.

Thus, based on the concept of effective elastic crack model, the critical values of K_{Ic} and $CTOD_c$ can be considered as the standard for fracture occurrence and the parameters for fracture characteristics of the concrete.

2.2 Cohesive crack model

Unlike the aforementioned effective elastic crack model, which overlooks all details of fracture progress occurring in the fracture progress zone and focuses on effective crack-tip only, the cohesive crack model traces all fracture progress zone. Cohesive crack, in this paper, means a hypothetical crack occurring in the crack progress zone, through which the stress at the crack surface is transferred as seen in Fig. 2.

The stress transferred by the cohesive crack can be expressed as a crack displacement Eq. (4) below.

$$\sigma = f(w) \tag{4}$$

where, $f(w)$ is a function of material characteristics as determined from an experiment. This function is called 'softening curve' and is be illustrated as in Fig. 3.

In the figure, G_F is the area under the softening curve and represents the fracture energy of the concrete, which is necessary to cause a crack per unit area. Fracture energy and softening curve are material characteristics, and there exist different

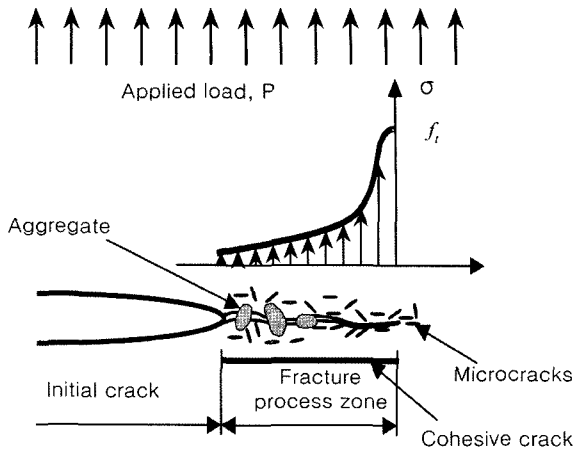

Fig. 2 Cohesive crack and fracture process zone.

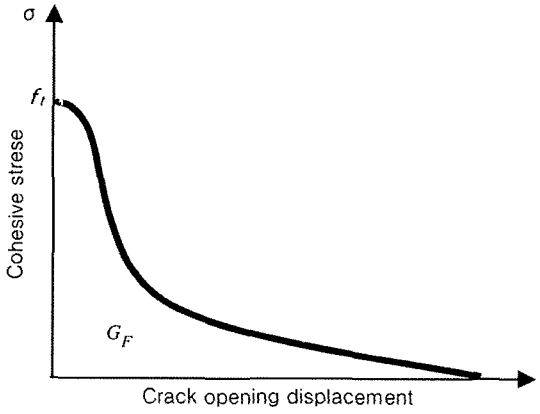

Fig. 3 Stress softening curve.

fracture energy and softening curve for each concrete. Thus, the fracture energy G_F and the softening curve can be regarded as fracture characteristics of concrete based on the concept of cohesive model.

3. Fracture experiment

3.1 Materials and mix design

The cement, fine aggregate, and coarse aggregate used in this experiment were domestically-produced Portland cement of first class, sand taken from the Geum river (specific gravity: 2.54, fineness modulus: 2.61), and crushed stones of 19 mm in maximum size (specific gravity: 2.59, fineness modulus: 6.27), respectively. Additionally, because high-strength concrete often causes poor workability, high performance water-reducing agent (super-plasticizer), which satisfies the standard of KS (Korean (Industrial) Standards) F 2560, was added to ensure the workability. The mix proportion of concrete to make the test specimen for wedge splitting test is given in Table 1.

Table 1 Mix proportion of concrete.

Water-cement ratio(%)	Fine aggregate ratio(%)	Unit weight(kg/m^3)				
		Water	Cement	Fine aggregate	Coarse aggregate	Super plasticizer
70	42	185	268	726	1,002	0.15%
55	42	185	342	727	1,030	0.3%
30	41	160	533	712	1,090	1%

3.2 Preparation of test specimens

This study selected a hexahedron for the shape of the test specimen to carry out wedge splitting tests for hexahedrons. A steel plate was inserted during concrete mixing, and the steel plate was removed after taken out of the cast to create the initial crack. A loading device with a roller was affixed, and a notch was cut out on the top of the test specimen to install displacement gauges. At the same time, cylindrical test specimens were also fabricated for the tests of compressive strength, modulus of elasticity, and tensile split.

The shape and size dimension of the hexahedron test specimen used in the wedge splitting test is shown in Fig. 4, and the specimen was taken out of the cast after 24 hours to treat it with wet curing prior to the experiment.

3.3 Experimental method

A wedge splitting test (WST) method as proposed by Bruhwiler[2] in 1988 was selected for this experiment. The wedge splitting test procedure is schematically presented in Fig. 5. After the test specimen with the notch at the top is placed on the supporter, the loading device with a roller is affixed at the upper part of the test specimen, and a high-strength steel plate with two wedges of same size and shape at its both sides is fixated above the loading device. As the wedges move between the roller at both sides, a vertical load is applied. The crack gauge installed on the axis of the roller and two locations along the crack surface measures the crack opening displacement (*COD*). The experiment is controlled by the crack opening displacement (*COD*) at the location of the roller axis. Just prior to the wedge splitting test, a compressive strength test and a test for modulus of elasticity was conducted, and the tensile strength test followed the specifications of KS F 2423 to measure the wedge split tensile strength.

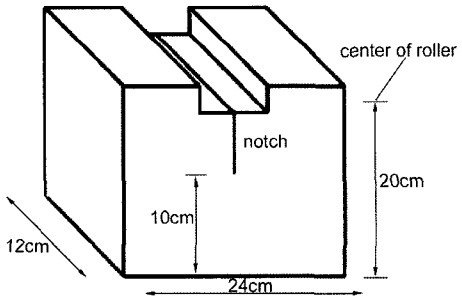

Fig. 4 Test specimen used in wedge splitting test.

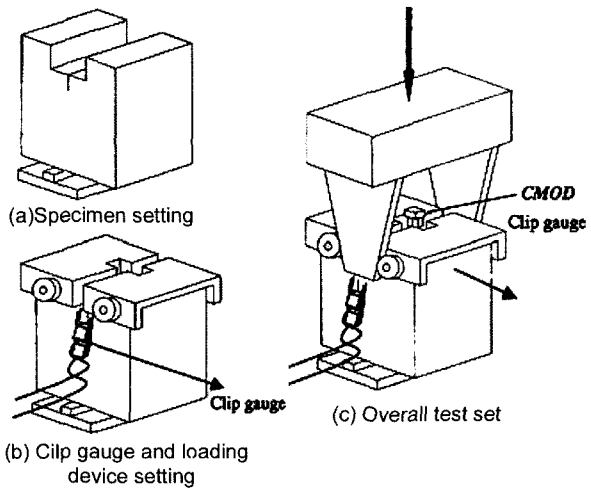

Fig. 5 Wedge splitting test procedure.

3.4 Experimental result

This paper denotes the low-strength, medium-strength, and high-strength specimens as LS, NS, HS, respectively, based on the experimental results. The properties of the concrete specimens as obtained from the compressive strength test and wedge split tensile strength test are provided in Table 2. Fig. 6 shows the load-crack mouth displacement (CMOD) curves as determined by the wedge splitting test for the concretes of three different strengths. The average values of crack opening displacement as measured at three locations of different distances apart from the crack tip under the peak load are shown in Fig. 7. Examining Fig. 6, the load increases as the crack opening displacement increases up to a certain point, and then the load drops abruptly. This shows that the crack grows stably only if the load is increased up to a critical point (the peak load). After this critical point, the crack grows unstably even if the load is decreased. This study assumed this critical point, at which the unstable crack growth begins, was the peak load as shown in Figs. 6, 7 shows that measured values at all three locations show a linearly increasing trend with the increased distance from the crack tip. This is construed to be due to the fact that the crack opening displacement follows the pattern of crack opening profile to be discussed in the next section.

4. Analysis and discussion

4.1 Analysis method

The length of effective elastic crack must be attained beforehand to obtain the critical stress intensity factor and critical crack-tip opening displacement as the fracture characteristics of concrete suggested by the effective elastic crack model. According to the two-parameter model of Jenq and Shah, unloading process must be conducted to attain the effective elastic crack length, which brings about the elastic deformation under the maximum load. Since it is very difficult to select the

Table 2 Proterties of concrete.

Type	Age (days)	Compressive strength (kgf/cm^2)	Tensile strength (kgf/cm^2)	Elastic modulus (10^5 kgf/cm^2)
LS	1	41	2.84	0.99
	3	106	15.7	1.77
	7	143	18.4	2.06
	14	157	24.8	2.14
	28	187	29.6	2.47
NS	1.5	58	15.9	1.33
	3.5	169	22.7	2.34
	7.75	226	33.3	2.68
	14.75	273	37.7	2.74
	28.5	338	40.0	2.96
HS	1	168	29.6	2.25
	3.25	266	39.3	3.03
	7.33	382	39.9	3.37
	14.75	533	46.8	3.43
	28	590	49.6	3.66

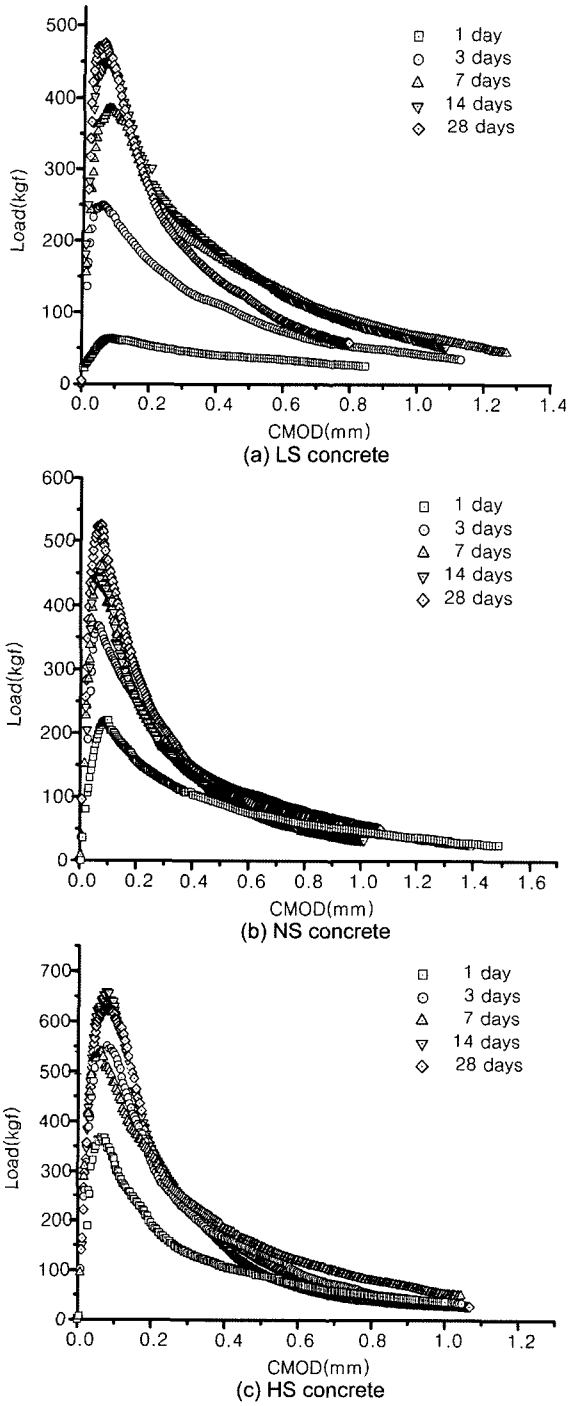

Fig. 6 Load-*CMOD* curves.

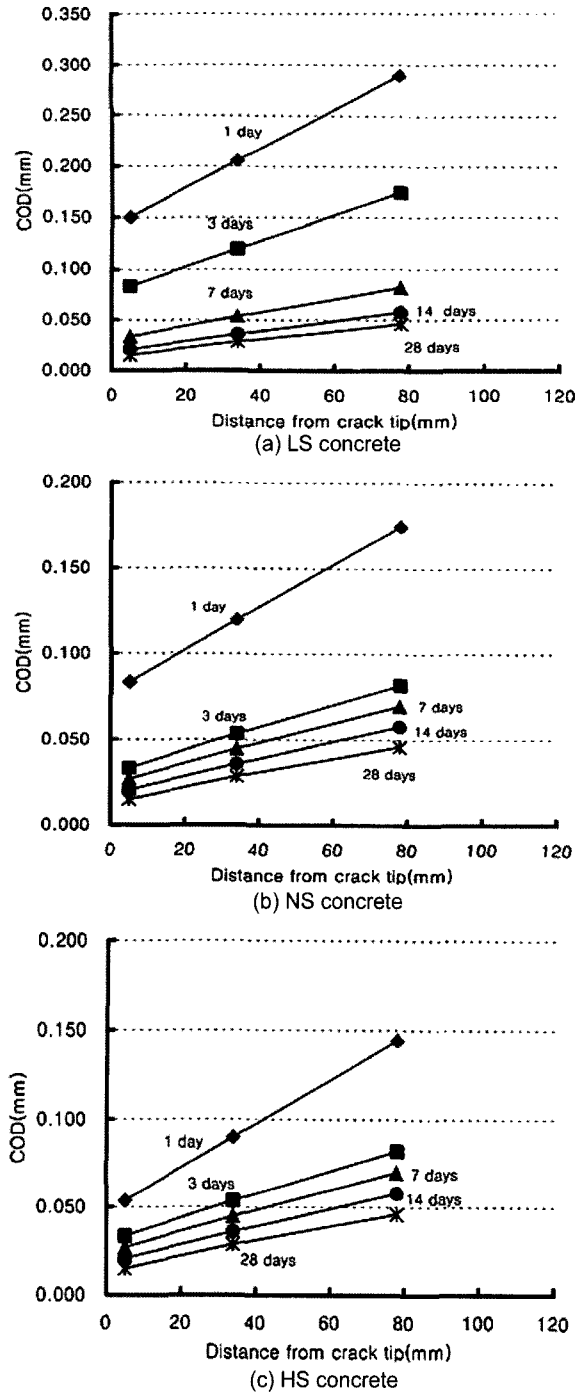

Fig. 7 Crack opening displacement at peak load.

point of unloading and its accompanied measurement of unloading gradient, this study bypassed the unloading process and used the crack opening profile, which is derived from linear elastic fracture dynamics, to predict the effective elastic crack length (α_e). This approach is expressed in Eq. (5) as follows.

$$COD(x, a) = CMOD \times g\left(\frac{a}{d}, \frac{x}{a}\right) \tag{5}$$

where, g is geometric function, α is the crack length, d is the depth of the test specimen, and x is the distance from the crack tip. In other words, Eq. (5) expresses the crack opening displacement (*COD*) as measured from the distance x as the crack mouth displacement (*CMOD*). Precisely speaking, although the g function of Eq. (5) differs by the pattern of the crack and the size and shape of the test specimen, the curve of g function is very similar for typical test specimens with ordinary edge crack.[3] This fact is illustrated in Fig. 8.

Examining Fig. 8, the effective crack length is non-linear around the crack tip and increases linearly as the distance from the crack tip increases. This concurs with the experimental results discussed in the previous section 3.4, which showed that the measured values for crack opening displacement at all three locations apart from the crack tip exhibited an increasing trend almost linearly with the increased distance from the crack tip. Thus, if these measured values for crack opening distance are substituted into Eq. (5), an equation for critical effective elastic crack length (α_{ec}) can be obtained. Given the critical effective elastic crack length, the initial crack length can be substituted

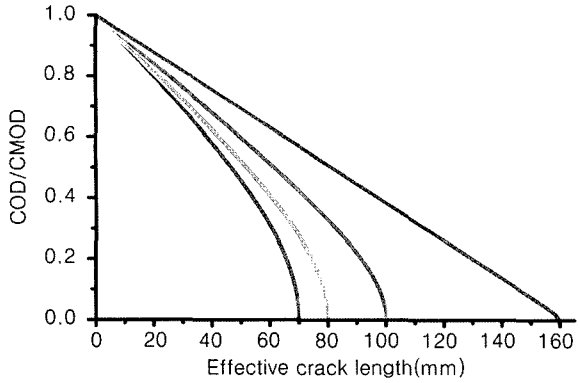

Fig. 8 Crack opening profile function for ordinary edge crack.

into x of Eq. (5) to obtain the critical crack-tip opening displacement ($CTOD_c$). Then, the effective elastic crack length and the peak load (P) are substituted into Eq. (6), which is suggested for compact tensile test specimens like those used in this experiment by ASTM, to compute the critical stress intensity factor (K_{Ic}).

$$K_I = \frac{P}{b\sqrt{d}} F\left(\frac{a}{d}\right) \tag{6}$$

where, $F(a/d)$ is a constant given by the initial crack length, b is the breadth (width) of the test specimen, and d is the depth of the test specimen.

Finally, the fracture energy G_F can be obtained by computing the area under the load-crack mouth displacement curve of Fig. 6.

4.2 Result of the analysis

The fracture characteristics obtained from the analysis of the experimental results are shown in Table 3 and Figs. 9~12. Examining the length of critical effective crack expansion in Fig. 9, the crack progresses more rapidly up until the peak period as the strength of the concrete is lower and the ages of the concrete is earlier. Additionally, as it can be conjectured from the crack opening profile function of Fig. 8, the critical crack-tip opening displacement ($CTOD_c$) of Fig. 10 exhibited the same trend as the aforementioned length of critical effective crack expansion to

Table 3 Fracture characteristics of concrete at early ages.

Type	Age (days)	$CTOD_c$ (mm)	K_{Ic} (Mpa m$^{1/2}$)	G_F (N/m)
LS	1	0.0628	0.6126	25.84
	3	0.0355	0.8907	101.31
	7	0.0292	1.0986	132.61
	14	0.0282	1.2579	132.60
	28	0.0272	1.4308	132.63
NS	1.5	0.0414	0.7694	93.11
	3.5	0.0302	1.0397	113.31
	7.75	0.0253	1.2430	130.22
	14.75	0.0233	1.3113	138.63
	28.5	0.0195	1.3327	173.14
HS	1	0.0309	1.1807	99.23
	3.25	0.0270	1.5254	126.19
	7.33	0.0237	1.4961	139.40
	14.75	0.0211	1.6123	139.91
	28	0.0179	1.6225	147.12

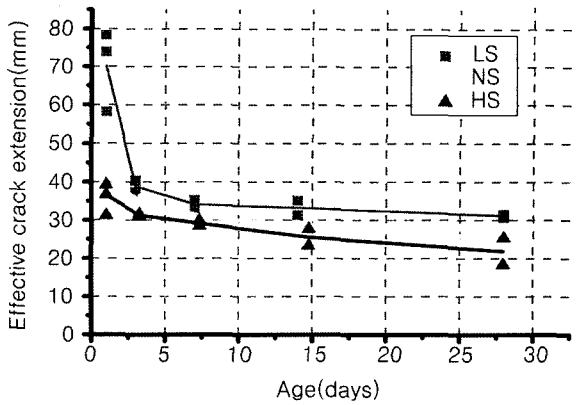

Fig. 9 Critical effective crack extension at various ages.

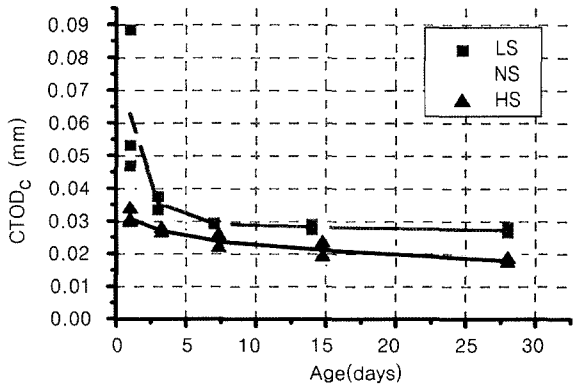

Fig. 10 $CTOD_c$ at various ages.

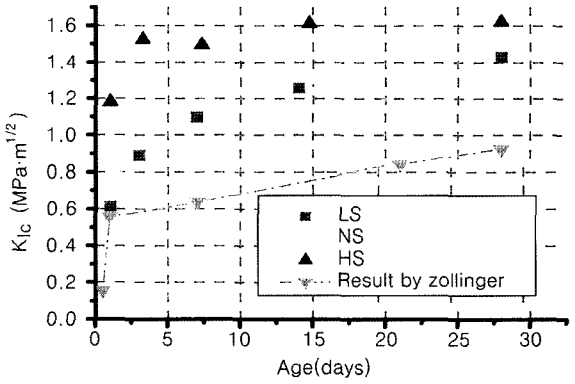

Fig. 11 K_{Ic} at various ages.

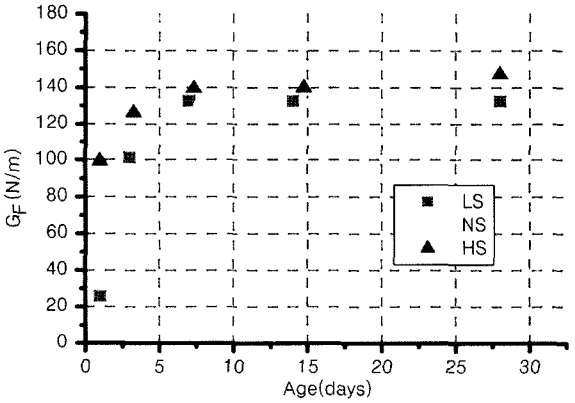

Fig. 12 G_F at various ages.

have higher values for lower strength and earlier ages of the concrete. The critical stress intensity factor (K_{Ic}) and the fracture energy (G_F), which are respectively depicted in Figs. 11 and 12, show a rapid increase during earlier ages and then start to converge to a certain extent at 28 days. This signifies sudden manifestation of strength and fracture toughness with the passage of time during earlier ages of the concrete. The results of Zollinger et al.,[4] who obtained the critical stress intensity factor at 0.5, 1, 7, 21, and 28 days through a 3-point flexural failure test, and Schutter et al.,[5] who reported the fracture energy of concrete at early ages, differed slightly from the results of this study. However, it is construed that they basically show the same trend as it is found in this study.

4.3 Reverse estimation of bilinear softening curve through a numerical analysis

Petersson[6] proposed a method to approximate the softening curve of concrete as previously shown in Fig. 3 with a bilinear curve as illustrated in Fig. 13. Thus, the estimation of the softening curve as a fracture characteristics of concrete can be simplified in terms of four parameter (f_t, f_1, w_1, w_c) estimation problem. This study carried out FEM (finite element analysis method) on the basis of the cohesive crack model for the test specimens used in the experiment on the basis of the principle of superposition as first suggested by Gopalaratnam[7] in 1991. The analysis crack with the application of the principle of superposition computes independent solutions for the elasticity against the outside load and the unit load, being applied along the crack surface of fracture progress zone. Then, these solutions are used to formulate a system of equations to satisfy the constraints (objective function) of the overall structural balance, appropriate conditions, and the relationship between bond stress and crack mouth displacement. This study assumed the stress condition as planar stress and divided the right half of the test specimen into 390 two-dimensional parabolic isoparametric elements as shown in Fig. 14. Then, 23 nodes were designated on the ligament of crack progress. These nodes were considered as nonlinear spring elements, which caused the bilinear softening phenomenon, to materialize the load-crack mouth displacement curve through FEM. The load-crack displacement curve so materialized can be obtained given the four parameters (f_t, f_1, w_1, w_c) of the bilinear softening curve. This study aimed to estimate optimally the bilinear softening curve, which could materialize the load-crack

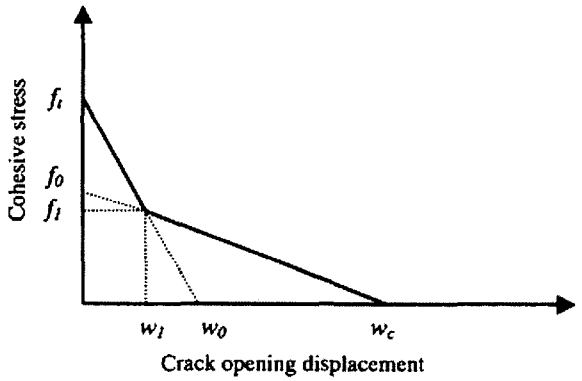

Fig. 13 Bilinear softening curve.

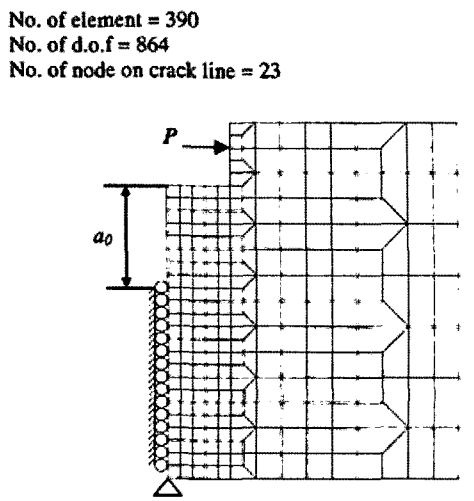

Fig. 14 Specimen configuration and finite element mesh.

mouth displacement relationship as previously depicted in Fig. 6.

The following function of four parameters as expressed in Eq. (7) can be conceived to compute the optimum solution.

$$F(f_t, f_2, w_1, w_c) = \int_0^{CMOD_0} (P_e - P_m)^2 d\delta \tag{7}$$

where, P_e is the load measured during the experiment, $CMOD_0$ is the crack mouth displacement at zero (no) load, and $P_m = P_m(f_t, f_1, w_1, w_c)$ is the load computed by FEM. Thus, the (error) function $F(f_t, f_1, w_1, w_c)$ numerically indicates the difference between the load-crack mouth displacement curve obtained from the experiment and that computed by the analysis. Thus, the most important standard for the evaluation of softening curve estimation may be claimed to be the values for $F(f_t, f_1, w_1, w_c)$. This value must be a positive number, and the condition for the minimum value of this function is given by the first-order differential Eq. (8) below.

$$\frac{\partial F}{\partial f_t} = \frac{\partial F}{\partial f_1} = \frac{\partial F}{\partial w_1} = \frac{\partial F}{\partial w_c} = 0 \tag{8}$$

Eq. (8) is basically a system of four nonlinear equations. Accordingly, this study employed a Newton-Raphson iteration method to solve (approximately) this system of four nonlinear equations. The problem-solving procedure is summarized in Fig. 15.[8-10] The differentials of the function $F(f_t, f_1, w_1, w_c)$ in shown in Fig. 15 can be approximated numerically as in Eq. (9).

$$\frac{\partial f}{\partial x} \approx \frac{f(x+h) - f(x-h)}{2h}$$

$$\frac{\partial^2 f}{\partial x^2} \approx \frac{f(x+h) + f(x-h) - 2f(x)}{h^2}$$

$$\frac{\partial^2 f}{\partial x \partial y} \approx \frac{f(x+h, y+g) + f(x-h, y-g)}{4hg}$$

$$\frac{f(x+h, y-g) + f(x-h, y+g)}{4hg} \tag{9}$$

The four parameters of bilinear softening curve obtained by the numerical analysis are summarized in Table 4 and are illustrated in Figs. 16 and 17. Examining Figs. 16 and 17,

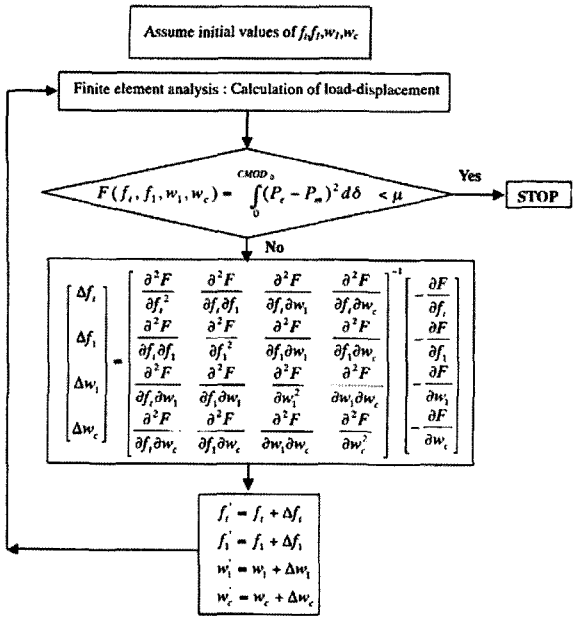

Fig. 15 Flow chart of the numerical procedure.

although there is a difference in magnitude by the strength, the increasing trend of f_t and f_1 and the decreasing trend of w_1 and w_c were observed with the increase in age of the concrete. This observation is explained by the fact that the load-crack mouth displacement curve increases with the age of the concrete up to the peak load and then a rapid softening phenomenon is observed after the peak load is reached. Additionally, the softening like other fracture characteristics of the concrete was manifested earlier as the strength of the concrete was higher.

In an ideal situation, the minium limit of the value for the error function $F(f_t, f_1, w_1, w_c)$ should be zero. However, due to various experimental and computational reasons, this value does not reach zero but have a certain positive value. Analyzing the experimental results summarized in Table 4, the average values of the error function $F(f_t, f_1, w_1, w_c)$ for LS, NS, and HS were computed to be 640.2 kgf^2 mm, 992.0 kgf^2 mm, and 1,965.6 kgf^2 mm, respectively. Considering that the limit value of the integral of $F(f_t, f_1, w_1, w_c)$ was assumed to be 2 mm, the average error for each value of CMOD on the load-crack mouth displacement curve (Fig. 6) was 17.9 kgf, 22.3 kgf, and 31.3 kgf for LS, NS, and HS concrete, respectively. The reason for this higher error with higher strength concrete is because the peak load on the load-crack mouth displacement curve is increased with higher strength concrete and then a rapid decrease in the load ensued right after the peak load. Since this study carried out the analysis with the same number of nodes on the ligament of crack progress for all three kinds of concrete strength, it can be

Table 4 Parameters of bilinear softening curve obtained by numerical analysis.

Type	Age (days)	f_t(Mpa)	f_1(Mpa)	w_1(mm)	w_c(mm)	$F(f_t, f_1, w_1, w_c)$ (kgf^{2}mm)
LS	1	0.272	0.193	0.072	0.324	12
	3	1.248	0.363	0.024	0.285	443
	7	2.079	0.616	0.023	0.271	1,053
	14	2.824	0.472	0.024	0.204	1,340
	28	2.964	0.643	0.013	0.186	353
NS	1.5	1.575	0.374	0.026	0.287	162
	3.5	1.816	0.366	0.028	0.228	973
	7.75	2.611	0.540	0.017	0.236	813
	14.75	3.296	0.489	0.010	0.196	892
	28.5	3.919	0.696	0.011	0.177	2,120
HS	1	2.881	0.383	0.024	0.186	527
	3.25	3.598	0.391	0.020	0.194	1,460
	7.33	4.381	0.561	0.017	0.156	2,727
	14.75	4.348	0.614	0.013	0.161	1,196
	28	4.711	1.082	0.007	0.117	3,918

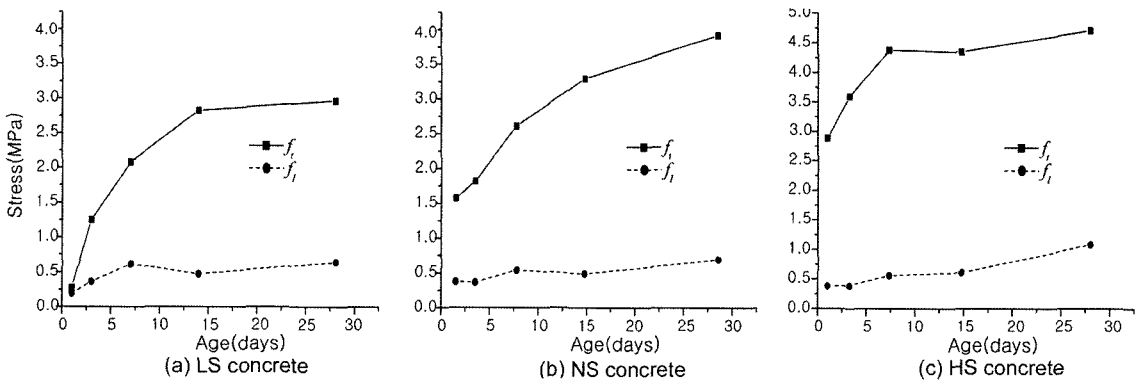

Fig. 16 Variation of parameter f_t, f_1.

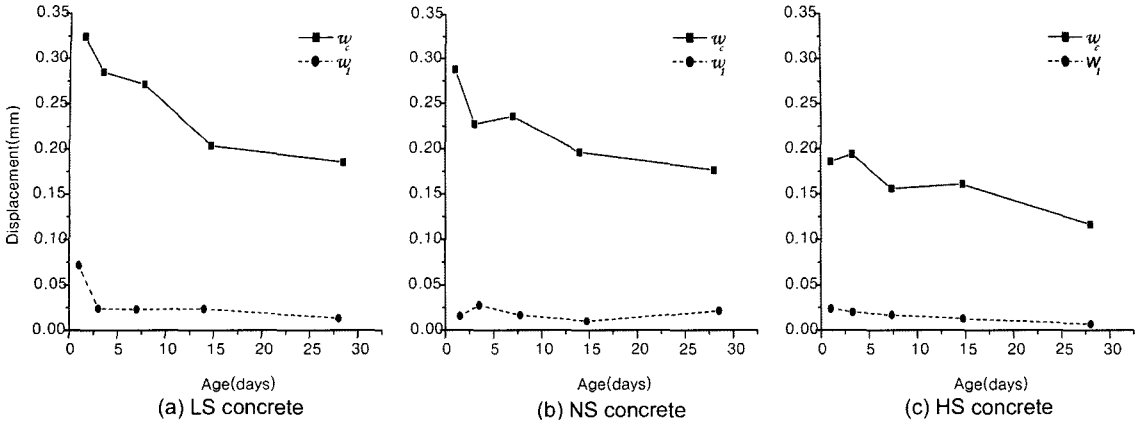

Fig. 17 Variation of parameter w_c, w_1.

reasoned that the error around the load shift will increase for higher strength concrete comparatively. On the other hand, if the number of nodes on the ligament of crack progress is increased for higher strength concrete, it is expected that the error will decrease. Additionally, this study employed the value of elastic modulus obtained from a cylindrical test specimen as an input constant for FEM in this research prior to the wedge splitting test. Thus, it follows that, if the modulus of elasticity, E, is added to the four parameters of the bilinear softening curve, f_t, f_1, w_1, w_c, as another unknown to be determined by a numerical analysis for five-parameters, then, it is expected that a more accurate load-crack mouth displacement curve will be obtained.

5. Conclusions

The following conclusions are derived from the experimental results of this study.

1) The length of critical effective elastic crack as defined by the effective elastic crack model could be attained by using the results of a more stable wedge splitting test and the crack opening profile while the unloading process during the experiment was bypassed.

2) Using the length of critical effective elastic crack aforementioned, the fracture characteristics of critical stress intensity factor and critical crack-tip opening displacement for the concrete at early ages are proposed. The critical stress intensity factor and the critical crack-tip opening displacement showed the tendency to increase and decrease, respectively, with the aging of the concrete up to the experimental period of 28 days.

3) The value for the fracture energy of the concrete at early ages was computed from the load-crack mouth displacement curve, which was obtained from a wedge splitting test. It exhibited the trend to increase with the aging of the concrete up to the experimental period of 28 days.

4) Based on the cohesive crack model, the bilinear softening curve for the concrete at early ages could be materialized (obtained) from a numerical analysis on the load-crack mouth displacement curve, which was computed by the FEM (Finite Element Method) on the test specimens of this study.

Acknowledgements

This research was supported by the research grant from the National Laboratory. The authors hereby express their sincere appreciation for the support.

References

1. Jenq, Y. S. and Shah, S. P., "A Two-Parameter Fracture Model for Concrete," *Journal of Engineering Mechanics*, Vol.111, No.4, 1985, pp.1227~1241.

2. Bruhwiler, E. and Wittmann, F. H., *The Wedge Splitting Test, A Method of Performing Stable Fracture Mechanics Tests*, Recent Publications, Ed. by Wittmann, F. H., 1988, pp.147~162.

3. Shah, S. P., Schwartz, E. S., and Ouyang, C., *Fracture Mechanics of Concrete*, John Wiley & Sons, 1995, pp.210~214.

4. Zollinger, D. G. and Tang, T., "Fracture Toughness of Concrete at Early Ages," *Materials Journal of ACI*, Vol.90, No.5, 1993, pp.463~471.

5. Schutter, G. D. and Taerwe, L., "Fracture Energy of Concrete at Early Ages," *Materials and Structures*, Vol.30, 1997, pp.67~71.

6. Petersson, P. E., *Crack Growth and Development of Fracture Zone in Plain Concrete and Similar Materials*, Report No. TVBM-1006, Division of Building Materials, Lund Institute of Technology, Lund, Sweden, 1981.

7. Gopalaratnam, V. S. and Ye, B. S., "Numerical Characterization of the Nonlinear Fracture Process in Concrete," *Engineering Fracture Mechanics*, Vol.40, No.6, 1991, pp.991~1006.

8. Wittmann, F. H., "Fracture Toughness and Fracture Energy of Concrete," *Proceedings of the International Conference on Fracture Mechanics of Concrete*, Lausanne, Switzerland, Elsevier, 1985, pp.163~175.

9. Mihashi, H. and Nomura, N., "Correlation between Characteristics of Fracture Process Zone and Tension-Softening Properties of Concrete," *Nuclear Engineering and Design*, Vol.165, pp.359~376, 1996.

10. Eo, S. H., Kim, J. G., and Kim, H. S., "Numerical Analysis of Fracture Characteristics and Size Effect of High-Strength Concrete Beams," *Journal of the Korean Society of Civil Engineers*, Vol.17, No.I-3, 1997, pp.361~371.

11. Kincaid, D. and Cheney, W., *Numerical Analysis*, Brooks/Cole Publishing Company, 1996, pp.499~511.